# EFFECT OF NONSTOICHIOMETRY ON DEFECT FORMATION IN SILICA GLASSES

Yoshimichi Ohki, Hiroyuki Nishikawa, Kaya Nagasawa*, and Yoshimasa Hama.

Department of Electrical Engineering, Waseda University, 3-4-1 Ohkubo, Shinjuku-ku, Tokyo 169, Japan.
*Department of Electrical Engineering, Shonan Institute of Technology, 1-1-25 Tsujido-Nishi-kaigan, Fujisawa, Kanagawa 251, Japan.

## ABSTRACT

Our studies on the effect of oxygen nonstoichiometry on the defect formation in silica glasses are reviewed. Defect species induced in pure-silica glasses by $\gamma$-ray or excimer-laser irradiation strongly depend on the nonstoichiometry, or the absolute deficiency or surplus of oxygen atoms to silicon atoms. That is to say, the lack of stoichiometry leads to the generation of either oxygen vacancies (≡Si-Si≡) or peroxy linkages (≡Si-O-O-Si≡) in as-manufactured pure-silica glasses. This was confirmed by ESR, optical absorption, photoluminescence, and theoretical calculations. For example, the oxygen vacancy has optical absorption bands at 5.0 and 7.6 eV, while the peroxy linkage at 3.8 eV. Since the 5.0- and 3.8-eV bands do not coexist in as-manufactured silicas, oxygen vacancy and peroxy linkage are considered not to be Frenkel defect

pair. Based on this fact, we classify low-OH silicas into two types, oxygen surplus and oxygen deficient. The excitation of either the 5.0 or 7.6-eV band results in the luminescence at 2.7 and 4.4 eV. The 2.7-eV luminescence is due to the triplet-to-singlet transition with a slow decay rate of $\tau \simeq 10$ ms, which is in agreement with the results of ab-initio molecular orbital calculation.

## 1. Classification of silica glasses

Fundamental defects in irradiated silicas such as the E'center, nonbridging oxygen hole center, and the peroxy radical have been identified by electron spin resonance (ESR)[1]. The formation mechanism of these defect centers suggest the existence of their own precursors.

E'centers are usually observed in any types of $\gamma$-irradiated silicas regardless of their OH contents. It has been proposed that E'centers can be formed by the hole trapping at the site of neutral oxygen vacancy[2]:

$$\equiv Si\text{-}Si\equiv \rightarrow \equiv Si\cdot + {}^{+}Si\equiv + e^{-} \qquad (1),$$

or the breaking of Si-H[3],

$$\equiv Si\text{-}H \rightarrow \equiv Si\cdot + \cdot H \qquad (2).$$

As has been called "wet OHC", NBOHCs are predominantly observed in high-OH silicas and their formation mechanism

have been thought as the fission of hydroxyl bond[4]:

$$\equiv Si\text{-}OH \rightarrow \equiv Si\text{-}O\cdot + \cdot H \qquad (3).$$

Also in low-OH silicas, the NBOHCs can be observed through the cleavage of peroxy linkage[5];

$$\equiv Si\text{-}O\text{-}O\text{-}Si\equiv \rightarrow \equiv Si\text{-}O\cdot + \cdot O\text{-}Si\equiv \qquad (4).$$

Peroxy radicals, previously called "dry OHC", can be formed by the hole-trapping on peroxy linkages[6]:

$$\equiv Si\text{-}O\text{-}O\text{-}Si\equiv \rightarrow \equiv Si\text{-}O\text{-}O\cdot + {}^{+}Si\equiv + e^{-} \qquad (5),$$

or by the reaction of E' centers with the oxygen molecules[7]:

$$\equiv Si\cdot + O_2 \rightarrow \equiv Si\text{-}O\text{-}O\cdot \qquad (6).$$

Strained Si-O-Si bond can be seen as the defect precursor and result in the radical pair of E'center and NBOHC[8]:

$$\equiv Si\text{-}O\text{-}Si\equiv \rightarrow \equiv Si\cdot + \cdot O\text{-}Si\equiv. \qquad (7)$$

From the left hand of the equations above, it is suggested that non-paramagnetic species such as $\equiv Si\text{-}Si\equiv$, $\equiv Si\text{-}O\text{-}O\text{-}Si\equiv$, $\equiv Si\text{-}OH$, and $\equiv Si\text{-}H$ should exist as precursors of radiation-induced defect centers. Among these, the presence of the $\equiv Si\text{-}OH$ and $\equiv Si\text{-}H$ groups can be detected by the IR absorption at $\simeq 3650 cm^{-1}$ and the Raman scattering at

2250cm$^{-1}$, respectively. Although UV absorption and photoluminescence measurement may detect these non-paramagnetic species, they lack structural information. Thus, the presence of the neutral oxygen vacancy and peroxy linkage has long been hypothetical.

It has been proposed that both oxygen vacancy and peroxy linkage exist as a Frenkel-defect pair[6] in as-manufactured silica, which are formed in the equilibrium during manufacturing process[9]:

$$2(\equiv Si\text{-}O\text{-}Si\equiv) \rightleftarrows \equiv Si\text{-}Si\equiv + \equiv Si\text{-}O\text{-}O\text{-}Si\equiv \quad (8).$$

On the other hand, the authors proposed that the oxygen vacancy and peroxy linkage are not Frenkel-type defects, and that the generation of these defects depends on the degree of oxidation, or the nonstoichiometry of silicon and oxygen atoms[10]. This is based on a fact that defect species induced by $\gamma$-irradiation or optical-fiber drawing in silica glass prepared under diverse oxygen concentrations show sample-to-sample variations. According to this view, silicas can be classified into two types: "oxygen-deficient" and "oxygen-surplus" silicas[11]. Oxygen-deficient silica can be defined as a silica in which oxygen vacancies presumably exist and drawing-induced E' centers can be observed. Oxygen-surplus silica is a silica in which peroxy linkages supposedly exist and peroxy radicals are observed after $\gamma$-irradiation or optical-fiber drawing.

If we assume the Frenkel-pair model, almost equal

numbers of E'centers and peroxy radicals should be observed according to Eqs. (1) and (5). As shown in Table I, however, in oxygen deficient silica, only E' centers are observed after γ-irradiation or fiber drawing. Thus, it is considered that the generation of oxygen vacancy and peroxy linkage is caused by the absolute deficiency or surplusage of the number of oxygen atoms to that of silicon atoms in silica.

## 2. Optical absorption and luminescence bands

### 2.1. Correlation of 5.0- and 7.6-eV bands with oxygen vacancy

$B_2$ band (5.0 eV) is one of the oldest known nonparamagnetic centers in a-$SiO_2$ whose exact structure has long been remained an open question. Twofold coordinated silicon (O-$\overset{\bullet}{\underset{\circ}{Si}}$-O)[12] and oxygen vacancy (≡Si-Si≡)[13] have been proposed as models for the $B_2$ band. The 7.6-eV band has been observed in neutron-irradiated[14] and in some types of silica glasses[3]. Based on theoretical calculations, several researchers identified 7.6-eV band with the oxygen vacancy[15,16].

However, it was not clear what relation the 7.6-eV band has with the 5.0-eV band, though both two bands have been identified with the oxygen vacancy (See Figs. 1 and 2).

The authors reported that drawing-induced E' centers are observed only in samples which exhibit the $B_2$ band[10]. Furthermore, the authors reported that there are two types of $B_2$ band, each with unique peak wavelength, half width,

photoluminescence spectra, and reaction to heat treatments (See Figs. 1 and 2)[17]. The $B_2$ bands were then classified into $B_2\alpha$ (5.0 eV) and $B_2\beta$ (5.1 eV).

On the oxygen vacancy defects, we performed ab-initio molecular orbital calculations using the model structure shown in Fig. 4[17,18]. The results shown in Fig. 5 indicate that the 7.6-eV band is due to the ground-to-singlet transition and 5.0-eV ($B_2\alpha$) band to ground-to-triplet transition. The much weaker intensity of the 5.0-eV band compared with 7.6-eV band reflects the forbiddenness of the transition from the singlet to triplet state. Moreover, a large decay constant of ≃10 ms supports the model, since calculation shows that the 2.7-eV band can be ascribed to triplet-to-singlet transition (See Fig. 5).

## 2.2. Relation between the 3.8-eV band and peroxy linkage

Relatively few things are understood on nonparamagnetic oxygen-surplus defects compared with the oxygen-vacancy defects. Although the presence of the peroxy linkage as a precursor of peroxy radical was suggested a decade ago, the absorption band related to peroxy linkages had not been reported until recent years.

Imai and coworkers identified a tail absorption band around 7 to 8 eV as the peroxy linkage in "oxygen-surplus" silica, which decreases by hydrogen treatment together with the growth of the OH group[3].

The authors[11] reported that an absorption band at 3.8 eV is seen only in "oxygen-surplus" low-OH silica as shown in

Fig. 6. Fig. 7 shows a good agreement between the decrease in 3.8-eV band and the growth of OH-group throughout a series of hydrogen treatment. Theoretical calculations[15] on peroxy linkages show that the transition energy from the oxygen's lone pair $p\pi^*$ orbital to the empty $p\sigma^*$ orbital is about 3.9 eV, quite similar to the 3.8 eV. We further found that the 3.8-eV band has grown by heat treatment at 900-1000 °C in oxygen gas. Based on these results, it is considered that the 3.8-eV band is due to peroxy linkages. However, on the 3.8-eV band, a very recent report[19] has shown that chlorine molecules dissolved in a glass network has a 3.8-eV band. So the assignment of the 3.8-eV band is still a matter of controversy.

## 2.3. Relation between the 1.9-eV luminescence and 4.8-eV absorption bands

The 1.9-eV luminescence band has several excitation bands, namely, at 2.0 eV[20,21], 4.8 eV[20,22,23], and 7.6 eV[24]. Some researchers proposed that both the 2.0-eV and 4.8-eV bands are ascribed to the NBOHCs, while others exclude the possibility of the NBOHC model for the 4.8-eV band. Figs. 8 (a) and (b) show the emission spectrum under 5.0-eV excitation and the excitation spectrum of 1.9-eV luminescence band, respectively. Our investigations on wide ranges of $\gamma$-irradiated silica have shown that the 1.9-eV luminescence band excited by the 4.8-eV band involves energy transfer between two different defects[25]. The energy acceptor defect, which is responsible for the 1.9 eV

luminescence, is NBOHC. The energy donor responsible for the 4.8 eV absorption is due to $\equiv Si-O^-$ defect. Contrary to this, an alternative model was recently proposed which involves a series of photochemical reactions, well established for gaseous oxygen: the 4.8-eV band is due to the Hartley band of $O_3$ molecules and the 1.9-eV band due to photodecomposition of $O_3$[26].

## 2.4. Spatial distribution of defects

The foregoing discussions involve the sample-to-sample variance of defect species and concentrations. In some cases, even a place-to-place dependence of the concentration of defects can be observed (See Fig. 9). In order to investigate this, we made a systematic study on the distribution of defects and impurities in high-purity silicas prepared by the plasma, soot, and direct methods[27]. The study on distribution is very important when investigating defects because the distribution should highlight the influence of preexisting defects and impurities on the induced defects.

## 2.5. Triplet-state defect and E'δ center in high-purity silica glass

Triplet state defect at $g \simeq 4$ and chlorine-related E'δ center were observed, for the first time by Griscom et al[28]. The following survey by the authors revealed several new features of both the triplet and E'δ center[29] (See

Fig. 10). Specifically, (i) oxygen vacancies, in addition to chlorine impurities, must be present for the defects to be induced, (ii) fluorine impurities can also give rise to these defects, and (iii) the termination of oxygen vacancies by hydrogen diffusion results in the suppression of these defects. These observations suggest that, whether a direct or indirect precursor, the oxygen vacancy is a requisite for the growth of these centers.

## 2.6. Generation mechanism of photoinduced paramagnetic centers from preexisting precursors in high-purity silicas.

The structures of the defect centers have been topics of researches for many years, but their generation mechanisms of defect centers had not been discussed in details, until recent two or three years[5,22,30-32]. The development of excimer lasers with UV or VUV output allows researchers a tunable excitation source for defect creation. For the past years, several workers made systematic studies using excimer lasers, such as photon energy dependence[33], irradiation temperature dependence[22], and power dependence[31,32]. With the exception of the intrinsic generation mechanism through the non-radiative decay of self-trapped exciton at high-power region[32], sample-to-sample variations which depend on the manufacturing conditions, are observed as in the case of ionizing radiation such as $\gamma$-rays. Therefore, it is important to use well-characterized silicas for the study of generation mechanism. In this view, we have

investigated wide ranges of samples which are characterized as mentioned above, and exposed them to 5.0 eV (KrF), 6.4 eV (ArF) and 7.9 eV ($F_2$) excimer lasers[5,34]. Sample dependences are seen as in the case of $\gamma$-irradiation, as shown in Fig. 11. The energy dependence is also observed for the induced-defect species. Namely, defects induced by 7.9-eV irradiation are different from those induced by 5.0- or 6.4-eV irradiation. From these observations, we proposed various generation processes based on the two-photon excitation model[31].

## 2.7. Various types of the NBOHCs

An absorption band is formed near 2 eV when silicas are subjected to $\gamma$-rays or other forms of radiations[35]. The defect responsible for the 2-eV band is considered NBOHC. Two different forms of NBOHCs were deconvoluted from the results of the isochronal annealing experiments[36]. Furthermore, it is found that excitation of these different 2-eV bands results in different luminescence peaks around 1.9 eV. The slight change in the absorption and luminescence peak energies is due to the change in the state of NBOHC. The forms of NBOHCs are material dependent and affected by either oxygen stoichiometry or hydroxyl content. Fig. 12 shows the energy diagram of various forms of nonbridging oxygen hole centers.

## 3. Summary

We have briefly reviewed our studies on the effects of nonstoichiometry on defect formation. We pointed out that significant attention should be paid also to oxygen non-stoichiometry on the defect formation, as well as impurity contents such as hydroxyls.

## Acknowledgments

Samples were partly provided by the courtesy of Shin-Etsu Quartz Products Co.,Ltd., and Shin-Etsu Chemical Co.,Ltd. This work was partly supported by a Grant-in-Aid for General Scientific Research (No.01460143) from the Ministry of Education, Science and Culture of Japan, by the Yazaki Memorial Foundation for Science and Technology, and by the Iketani Science and Technology Foundation.

## References

1. D.L. Griscom, in Defects in Glasses, Vol.61 of Materials Research Society Symposium Proceedings, edited by F.L. Galeener, D.L. Griscom, and M.J. Weber, (MRS, Pittsburgh, PA, 1986), p. 213.

2. F.J. Feigl, W.B. Fowler, and K.L. Yip, Solid State Commun. 14, 225 (1974).

3. H. Imai, K. Arai, T. Saito, S. Ichimura, H. Nonaka, J.P. Vigouroux, H. Imagawa, H. Hosono, and Y. Abe, in The Physics and Technology of Amorphous $SiO_2$, edited by R.A.B. Devine (Plenum, New York, 1988), p.153.

4. M. Stapelbroek, D.L.Griscom, E.J. Friebele, and

G.H. Sigel, Jr., J. Non-Cryst. Solids 32, 313 (1979).

5. H. Nishikawa, R. Nakamura, R. Tohmon, Y. Ohki, Y. Sakurai, K. Nagasawa, and Y. Hama, Phys. Rev. B 41, 7828 (1990).

6. E.J. Friebele, D.L. Griscom, M. Stapelbroek, and R.A. Weeks, Phys. Rev. Lett. 42, 1346 (1979).

7. A.H. Edwards and W.B. Fowler, Phys. Rev. B26, 6649 (1982)

8. S. Munekuni, N. Dohguchi, H. Nishikawa, K. Nagasawa, Y. Ohki, and Y. Hama. Extended Abstracts of the 51st Annual Meeting of The Japan Society of Applied Physics 1990, Vol.2, 26p-MF-16, p.719 (in Japanese).

9. J. Robertson, J. Phys. C. 17, 221(1984).

10. K. Nagasawa, Y. Hoshi, and Y. Ohki, Jpn. J. Appl. Phys., 26, L554 (1987).

11. H. Nishikawa, R. Tohmon, Y. Ohki, K. Nagasawa, and Y. Hama, J. Appl. Phys. 65, 4672 (1989).

12. L.N. Skuja, A.N. Streletsky, and A.B. Pakovich, Solid State Commun. 50, 1069 (1984).

13. G. W. Arnold, IEEE Trans. Nucl. Sci. NS-20, 220 (1973).

14. C.M. Gee and M.A. Kastner, Phys. Rev. Lett. 42, 1765 (1979).

15. E.P. O'Reilly and J. Robertson, Phys. Rev. B, 27, 3780 (1983).

16 D.L. Griscom, J. Non-Cryst. Solids 73, 51 (1985).

17. R. Tohmon, H. Mizuno, Y. Ohki, K. Sasagane, K. Nagasawa, and Y. Hama, Phys. Rev. B, 39, 1337 (1989).

18. R. Tohmon, Y. Shimogaichi, H. Mizuno, Y. Ohki, K. Nagasawa, and Y. Hama, Phys. Rev. Lett. 62, 1388 (1989).

19. K. Awazu, H. Kawazoe, and K. Muta, in Ref.8, 27p-MF-14, p.718 (in Japanese).

20. L.N. Skuja and A.R. Silin, Phys. Status Solidi A 56, K11 (1979).

21. G.H. Sigel and M.J. Marrone, J. Non-Cryst. Solids 45, 235 (1981).

22. R.A.B. Devine, in Ref. 1, p. 177.

23. J.H. Stathis and M.A. Kastner, Philos. Mag. B49, 357 (1984).

24. J.H. Stathis and M.A. Kastner, Phys. Rev. B35, 2972 (1987).

25. R. Tohmon, Y. Shimogaichi, S. Munekuni, Y. Ohki, Y. Hama, and K. Nagasawa, Appl. Phys. Lett. 54, 1650 (1989).

26. K. Awazu and H. Kawazoe, J. Appl. Physics, 68, 3584 (1990).

27. R. Tohmon, A. Ikeda, Y. Shimogaichi, S. Munekuni, Y. Ohki, K. Nagasawa, and Y. Hama, J. Appl. Phys. 67, 1302 (1990).

28. D.L. Griscom and E.J. Friebele, Phys. Rev. B 34, 7524 (1986).

29. R. Tohmon, Y. Shimogaichi, S. Munekuni, Y. Ohki, Y. Hama, and K. Nagasawa, Phys. Rev. B 41, 7258 (1990).

30 H. Imai, K. Arai, H. Imagawa, H. Hosono, and Y. Abe, Phys. Rev. B 38, 12772 (1988).

31 K. Arai, H. Imai, H. Hosono, Y. Abe, and H. Imagawa, Appl. Phys. Lett. 53, 1891 (1988).

32. T.E. Tsai, D.L. Griscom, and E.J. Friebele, Phys. Rev. Lett. 61, 444 (1988).

33. J.H. Stathis and M.A. Kastner, Phys. Rev. B 29, 7079 (1984).

34. R. Nakamura, H. Sugisawa, H. Nishikawa, Y. Ohki,

Y. Hama, and K. Nagasawa, in Ref. 8, 26p-MF-10, p. 707 (in Japanese).

35. K. Nagasawa, Y. Ohki, and Y. Hama, Jpn. J. Appl. Phys. 26, L1009 (1987).

36. S. Nunekuni, T. Yamanaka, Y. Shimogaichi, R. Tohmon, Y. Ohki, K. Nagasawa, and Y. Hama, J. Appl. Phys. 68, 1212 (1990).

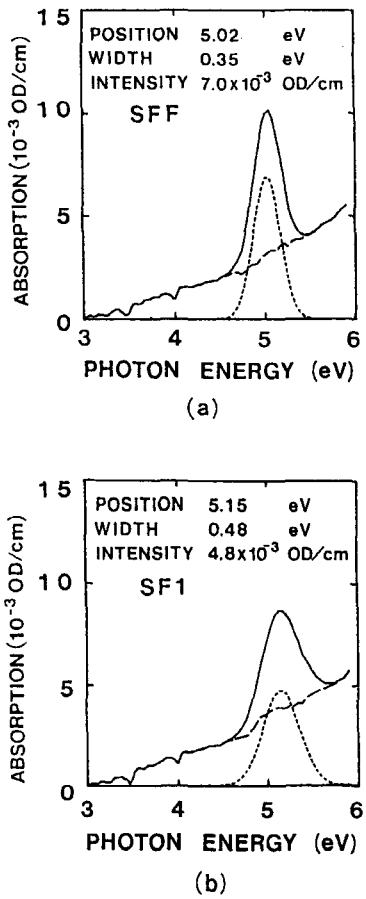


FIG. 1. Optical-absorption spectra: (a) $B_2$ $\alpha$-type (SFF) and (b) $B_2$ $\beta$-type (SF1) silicas. Solid line: experimental data, dotted line: fitted Gaussian curve using parameters given at the top of figure, broken line: result of subtracting Gaussian curve from experimental curve.

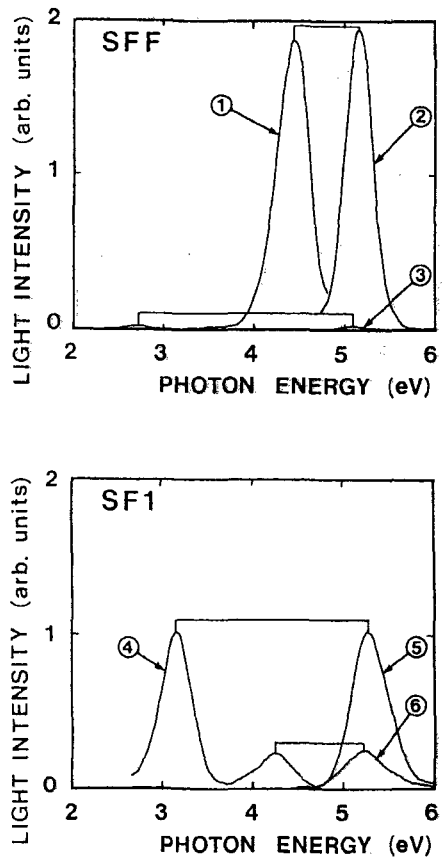


FIG. 2. Photoluminescence spectra: (a) $B_2\alpha$-type and (b) $B_2\beta$-type silicas. 1 and 4: emission spectra under 5.06-eV excitation, 2: excitation spectrum of 4.42-eV PL band ($B_2\alpha$). 3: excitation spectrum of 2.74-eV PL band ($B_2\alpha$), 4: excitation spectrum of 3.16-eV PL band ($B_2\beta$), 6: excitation spectrum of 4.24-eV PL band ($B_2\beta$).

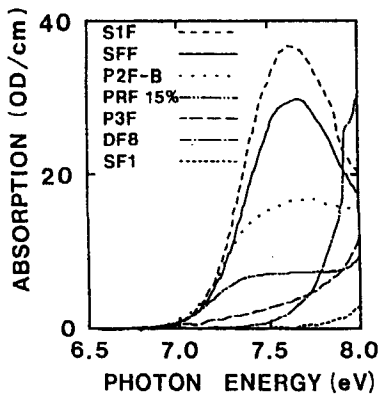


FIG. 3. Vacuum-uv optical-absorption spectra of various samples.

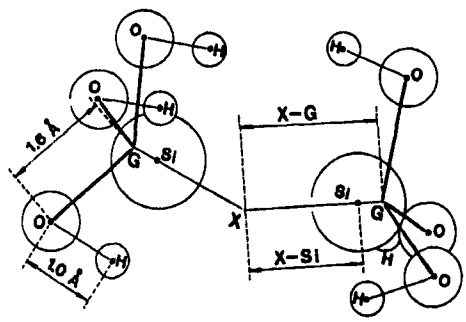


FIG. 4. Model structure for numerical calculation.

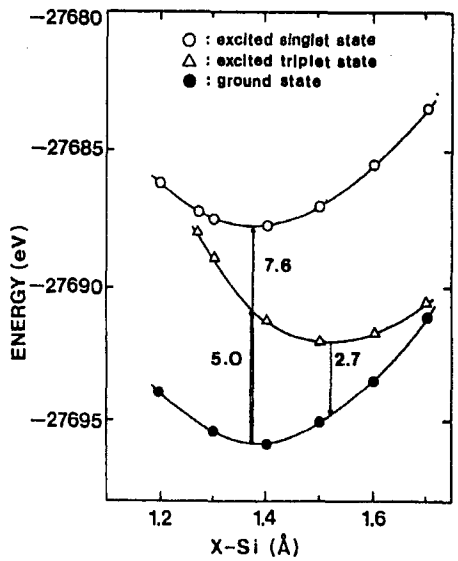


FIG. 5. Calculated energy values of the oxygen vacancy in the various states.

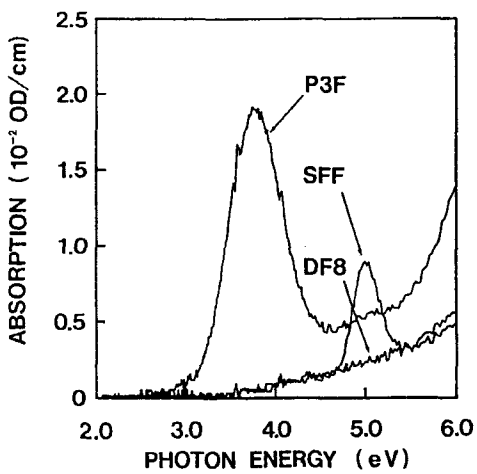


FIG. 6. UV absorption spectra of three types of samples: high-OH DF8, oxygen-deficient SFF, and oxygen-surplus P3F.

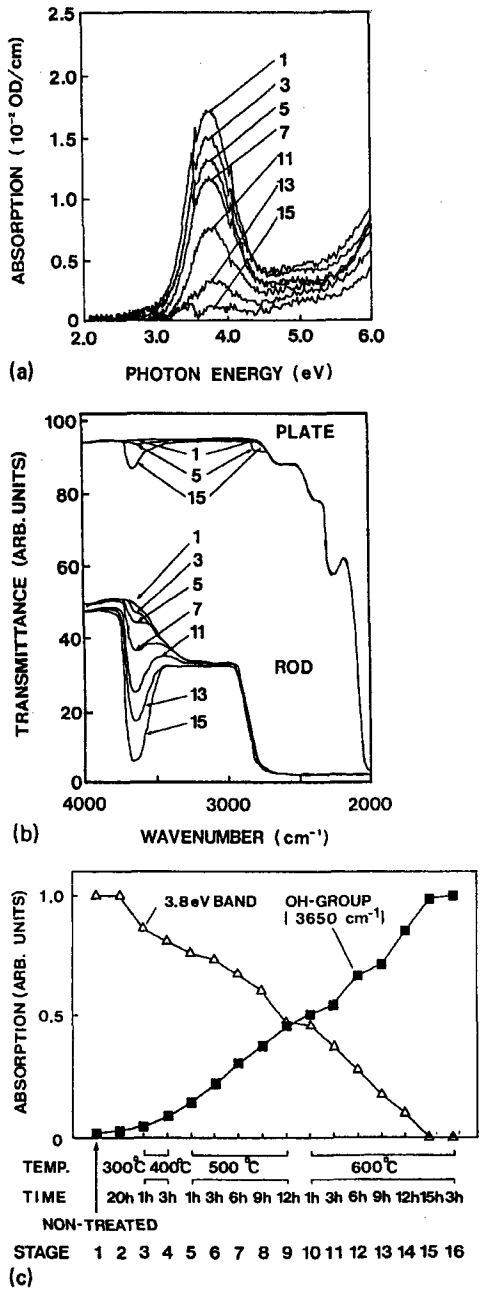


FIG. 7. Change in absorption by a series of hydrogen treatments done on oxygen-surplus silica. (a) UV spectra of the rod-shaped sample, (b) IR spectra of the rod and plate samples, and (c) the 3.8-eV band intensity and OH-group absorption at 3650$cm^{-1}$ of the rod sample.

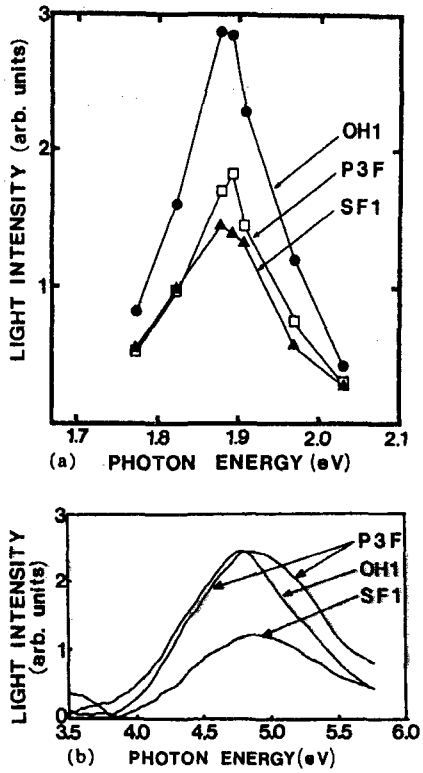


FIG. 8. Photoluminescence spectra of the 1.9-eV band excited by the 4.8-eV excitation band. (a) Emission spectrum under 5.0-eV excitation. (b) Excitation spectrum of 1.9-eV luminescence band.

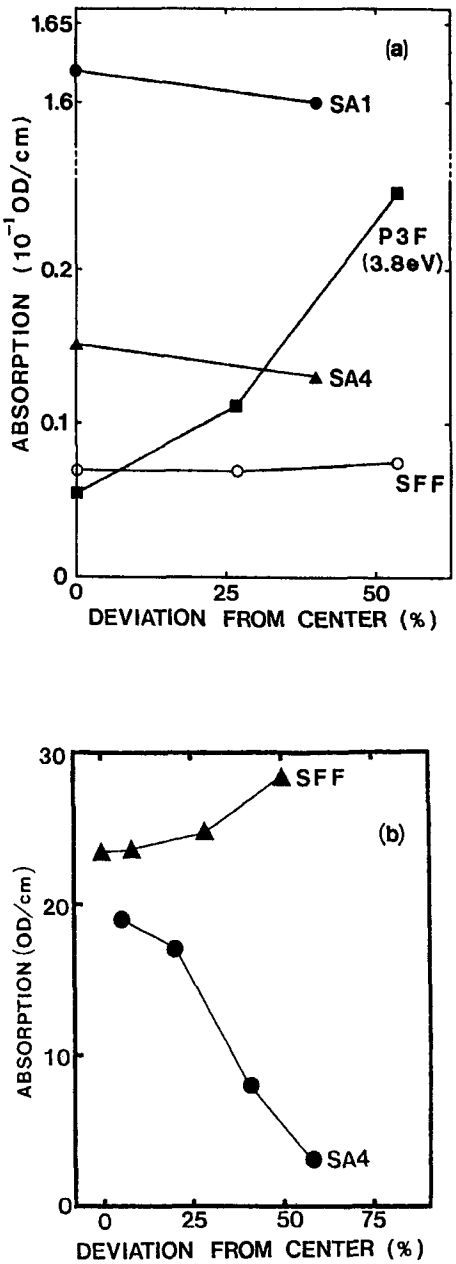


FIG. 9. Radial distribution of optical absorption. (a) Distribution of the 3.8-eV band for oxygen-surplus silica (P3F) and the $B_2\alpha$ (5.0 eV) band for oxygen deficient silicas (SA1, SA4, and SFF).

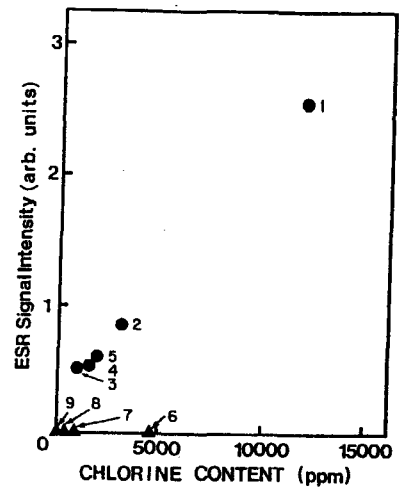


FIG. 10. ESR signal intensity of the triplet as a function of chlorine content. Note the impurity in the sample 5 is fluorine.

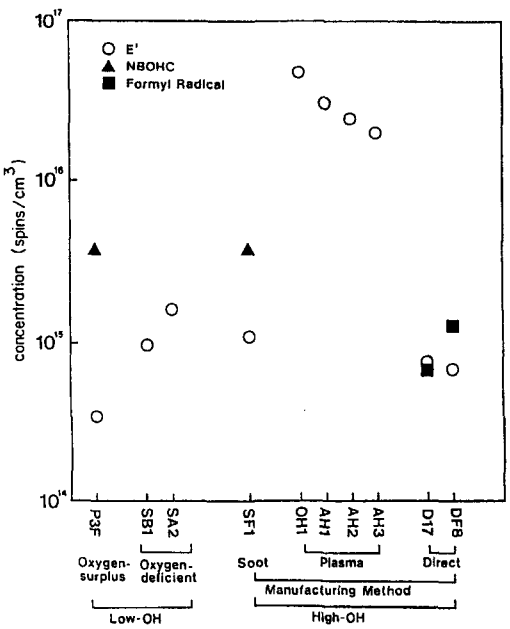


FIG. 11. Concentrations of paramagnetic centers (○:E' centers, ▲:NBOHC, ■:formyl radical) induced by ArF-excimer laser irradiation in low-OH (oxygen-surplus P3F, oxygen-deficient SA2 and SB1), $B_2\beta$-type (SF1), and high-OH (OH1, AH1, AH2, and AH3, DF8 and D17) silicas.

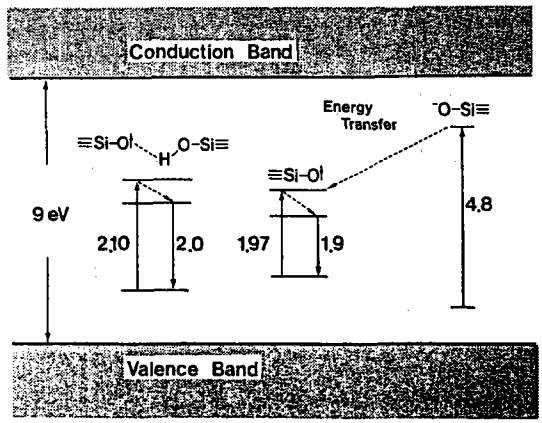


FIG. 12. Energy diágram of various forms of nonbridging oxygen hole centers.